Optimization of Multi-layer Active Magnetic Regenerator towards Compact and Efficient Refrigeration

Lei, Tian; Engelbrecht, Kurt; Nielsen, Kaspar Kirstein; Neves Bez, Henrique; Veje, Christian T.; Bahl, Christian

Published in:
Proceedings of the 29th International Conference on Efficiency, Cost, Optimisation, Simulation and Environmental Impact of Energy Systems (ECOS 2016)

Publication date:
2016

Document Version
Peer reviewed version

Optimization of Multi-layer Active Magnetic Regenerator towards Compact and Efficient Refrigeration

Tian Lei[a], Kurt Engelbrecht[a], Kaspar K. Nielsen[a], Henrique Neves Bez[a], Christian T. Veje[b], Christian R. H. Bahl[a]

[a] *Technical University of Denmark, Roskilde, Denmark, tile@dtu.dk*
[b] *University of Southern Denmark, Odense, Denmark*

Abstract:

Magnetic refrigerators can theoretically be more efficient than current vapor compression systems and use no vapor refrigerants with global warming potential. The core component, the active magnetic regenerator (AMR) operates based on the magnetocaloric effect of magnetic materials and the heat regeneration processes of periodic fluid blows. Magnetocaloric materials with a first order phase transition (FOPT) are suitable to realize a higher cooling capacity than commonly used gadolinium, but layering such materials is necessary, due to a large isothermal entropy change (ΔS_m) in a narrow region around their Curie temperature. Simulations are implemented to investigate how to layer the FOPT materials for obtaining higher cooling capacity. Moreover, based on entropy generation minimization, optimization of the regenerator geometry and related operating parameters is presented for improving the AMR efficiency. In addition, simulations are carried out to investigate the potential of applying nanofluid in future magnetic refrigerators.

Keywords:

Magnetic refrigeration, Magnetocaloric material, Regenerator optimization, Nanofluid

1. Introduction

Room temperature magnetocaloric refrigerators (MCR) operate based on the magnetocaloric effect (MCE) and principle of heat regeneration. Compared to a vapor compression refrigerator, MCRs exhibits advantages such as high theoretical efficiency, avoiding use of vapor refrigerants, and easy integration with distributed heat exchangers. Therefore, an MCR is considered to be a compact and efficient refrigeration technology and attracts a lot of attentions in recent decades. Tura and Rowe presented the improvements of a prototype, which can realize a maximum no-load temperature span of 29 ºC and a cooling power of 50W at 2 ºC temperature span [1]. Engelbrecht et al. [2] built a rotary MCR and it exhibits a no-load temperature span of over 25 ºC and a maximum cooling power of 1010 W using gadolinium (Gd) spheres. Jacobs et al. [3] presented a rotary prototype using six layers of LaFeSiH particles, producing 3042 W cooling power at zero temperature span and 2502 W over a span of 12ºC with a coefficient of performance (COP) around 2. A compact rotary MCR presented by Eriksen et al. [4] could realize a temperature span of 10.2 ºC at a cooling load of 103 W and a COP of 3.1. More prototypes and materials are reviewed in References [5-7].

The magnetocaloric effect can be explained from the viewpoint of thermodynamics. Upon an increase in the applied magnetic field, the magnetic contribution to the entropy (S_m) of the magnetocaloric material (MCM) will decrease. Under an adiabatic condition, this magnetization process leads to an increase in temperature, which is so called adiabatic temperature change ΔT_{ad}, since the lattice and/or electronic contributions to the entropy must increase to hold the total entropy constant [6]. While in an isothermal process, the total entropy change of MCM is equal to the magnetic entropy change ΔS_m. The intensity of the MCE is largest when the temperature approaches the material's Curie temperature T_{Curie} and increases with increasing magnetic field

change. Assuming no magnetic hysteresis, the magnetization and demagnetization processes are considered reversible, which indicates that an MCR can realize high theoretical efficiency.

Permanent magnets are commonly used in existing room temperature MCR devices and the reachable magnetic field of a typical permanent magnet is of the order 1.5 T. Upon this magnetic field change, the adiabatic temperature change for the best performing materials will be about 5 ºC [6,7]. It is, however, not enough for most applications, such as domestic refrigeration. Therefore, the principle of heat regeneration and the AMR [8] are necessary to increase the temperature span to an applicable level. An AMR is a solid porous matrix consisting of the magnetocaloric materials, where a heat transfer fluid may flow through and exchange heat with the solid. As shown in Figure 1, a typical AMR cycle comprises four steps: (a) adiabatic magnetization associated with an increase in the solid temperature T_s; (b) cold-to-hot blow, where T_s decreases due to heat transfer with the fluid; (c) adiabatic demagnetization, and T_s further decreases below the initial state; (d) hot-to-cold blow, and the solid absorbs heat from the heat transfer fluid, leading to a lower temperature in the outflow than the load temperature at the cold end. Driven by this temperature difference, the fluid can absorb a certain amount of heat, i.e., cooling power, from the load. After several cycles, a temperature gradient larger than ΔT_{ad} can be built up between the hot and cold ends, and the magnetocaloric materials along the regenerator work in different temperature regions based on location.

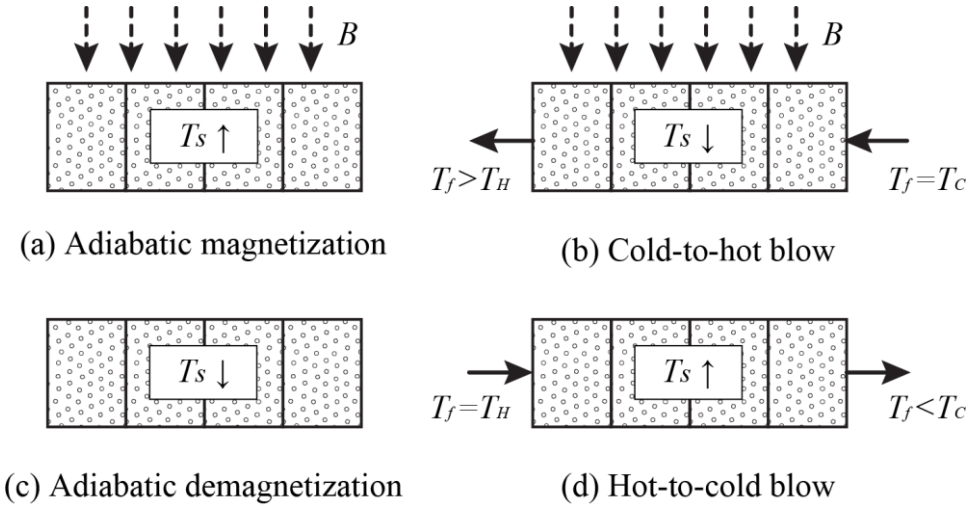

Figure 1. A typical cycle of multi-layer magnetic regenerator

Materials with a large MCE are key factors for an MCR to realize compact and efficient refrigeration. Compared with magnetocaloric materials with a second order phase transition (SOPT) such as Gd, MCMs with a first order phase transition (FOPT) exhibit a larger peak value in ΔS_m near T_{Curie}. This may be beneficial for elevating the specific cooling power, which is the cooling power per kilogram of MCM. Applying FOPT materials in future prototypes is promising; however, a previous study [9] showed that 2.2 layers per 5 ºC temperature span are needed for regenerators using the FOPT material $La(Fe,Mn,Si)_{13}H_y$. Comparing AMRs using first and second order magnetocaloric materials is thus of substantial interest and we present a study by simulation based on a one dimensional (1D) model. The influences of the number of layers and the temperature span on the specific cooling power are quantified. Based on analysis, a practical number of layers is proposed to reach 90% of the theoretical specific cooling power.

Besides maximizing the magnetocaloric properties, minimizing the losses inside the AMR is important for improving the refrigeration efficiency. According to a previous study [10], the main losses are caused by the insufficient heat transfer between the fluid and solid refrigerant as well as at the hot or cold heat exchangers, viscous dissipation due to the pump work and axial conduction.

These three loss mechanisms are directly or indirectly related to the regenerator geometry and operating parameters, including the frequency, fluid flow rate, aspect ratio and hydraulic diameter. To minimize the total loss and maximize the COP, a multi-parameter optimization of AMRs using a packed sphere bed is presented. Furthermore, entropy production rates are calculated and compared for quantitative analysis of the impacts of different loss mechanisms.

Aqueous solutions with anti-corrosion additives are widely used in existing MCR devices as heat transfer fluids, and the additives usually have a lower thermal conductivity and higher viscosity than water, which reduces efficiency. Although many studies have been carried out to enhance the heat transfer performance using nanofluids [11], which is produced by suspending nanoparticles in base fluids, investigation of applying nanofluids in the regenerator or the AMR is rarely reported. In this study, the performance of an AMR using nanofluid containing titania nanosheets (TNS) is predicted and compared with water and aqueous solution with 20% v/v ethylene glycol (EG) based on simulation.

2. Numerical model

To investigate the active magnetic regenerator, a one dimensional transient numerical model [10] is used. Considering the conduction, enthalpy flow, heat transfer between fluid and solid, viscous dissipation, energy storage and magnetic work, the governing equations for the heat transfer liquid and solid refrigerant are:

$$\frac{\partial}{\partial x}\left(k_{disp}\frac{\partial T_f}{\partial x}\right)A_c - \dot{m}_f c_f \frac{\partial T_f}{\partial x} - \frac{Nuk_f}{d_h}a_s A_c\left(T_f - T_r\right) + \left|\frac{\partial P}{\partial x}\frac{\dot{m}_f}{\rho_f}\right| = \rho_f A_c \varepsilon c_f \frac{\partial T_f}{\partial t} \quad (1)$$

$$\frac{\partial}{\partial x}\left(k_{stat}\frac{\partial T_r}{\partial x}\right)A_c + \frac{Nuk_f}{d_h}a_s A_c\left(T_f - T_r\right) = A_c(1-\varepsilon)\rho_r\left[c_{\mu_0 H}\frac{\partial T_r}{\partial t} + T_r\left(\frac{\partial s_r}{\partial H}\right)_T\frac{\partial H}{\partial t}\right] \quad (2)$$

where k, T, ρ, c and s are the thermal conductivity, temperature, density, specific heat and specific entropy; A_c, x, t, $\dot{m}_f$ and H are the cross sectional area, axial position, time, mass flow rate and internal magnetic field. The subscripts f and s represent fluid and solid refrigerant, respectively.

The central difference and implicit time schemes are used for discretizing the governing equations in both space and time domains. Given the initial temperature, mass flow rate and applied magnetic field, the fluid and solid temperatures can be solved at each time step. After reaching a periodical steady state with a specified tolerance, the simulation will be terminated and the indices, such as cooling power and COP, are output. In the simulation, the number of the space and time nodes is 100 and 4000 respectively. More details for the expressions of thermal conductivity due to fluid dispersion, static thermal conductivity, pressure drop and Nusselt number are described in Ref. [12].

According to the second law of thermodynamics, the entropy production of an irreversible thermal process $\dot{S}_p$ is larger than zero, and for a reversible process $\dot{S}_p = 0$. The entropy production can be used to evaluate the irreversibility and the method of entropy production minimization is widely utilized to optimize the thermal system. Considering an amount of heat $\Delta Q = kAdT/dx$ is transferred between two adjacent elements with temperature T_1 and $T_2 (T_1 > T_2)$. The entropy changes in both sides are $-\Delta Q/T_1$ and $\Delta Q/T_2$, resulting in a total entropy change of $-\Delta Q/T_1 + \Delta Q/T_2 = \Delta Q(T_1 - T_2)/T_1 T_2$, which is also the entropy production of this process for an isolated system. Based on the numerical model, the entropy production due to insufficient heat transfer, viscous dissipation and axial conduction are calculated in Eqns. 3-6[10,13]:

$$\dot{S}_{p,ht} = \frac{1}{\tau}\int_0^\tau\int_0^L h a_s A_c \frac{\left(T_f - T_s\right)^2}{T_f T_s}dxdt + \frac{1}{\tau}\int_0^\tau \left|\dot{m}_f\right| c_f\left(\ln\frac{T_C}{T_{f,x=L}} + \frac{T_{f,x=L} - T_C}{T_C} + \ln\frac{T_H}{T_{f,x=0}} + \frac{T_{f,x=0} - T_H}{T_H}\right)dt \quad (3)$$

$$\dot{S}_{p,vd} = \frac{1}{\tau}\int_0^\tau \int_0^L \frac{|\dot{m}_f|}{\rho_f T_f}\frac{\partial P}{\partial x}\,dxdt \quad (4)$$

$$\dot{S}_{p,ac} = \frac{1}{\tau}\int_0^\tau \int_0^L \left[k_{stat}A_c\frac{1}{{T_s}^2}\left(\frac{dT_s}{dx}\right)^2 + k_{disp}A_c\frac{1}{{T_f}^2}\left(\frac{dT_f}{dx}\right)^2\right]dxdt \quad (5)$$

$$\dot{S}_{p,tot} = \dot{S}_{p,ht} + \dot{S}_{p,vd} + \dot{S}_{p,ac} \quad (6)$$

where $\dot{S}_{p,ht}$, $\dot{S}_{p,vd}$ and $\dot{S}_{p,ac}$ are the entropy production rates due to insufficient heat transfer, viscous dissipation and axial conduction, respectively; $\dot{S}_{p,tot}$ is the total entropy production rate; L and τ are the regenerator length and the cycle period.

3. Results and discussion

3.1. Multi-layer regenerator using magnetocaloric material with FOPT or SOPT

In a multi-layer AMR, various magnetocaloric materials with different T_{Curie} are aligned along the regenerator following the temperature gradient. For modeling such a multi-layer AMR, the entropy data as a function of the internal magnetic field and temperature of numerous materials are needed. It is assumed that those entropy data can be obtained by shifting the measured data of the base material according to the designed T_{Curie}. Here La(Fe,Mn,Si)$_{13}$H$_y$ with T_{Curie}=31.8 ºC and Gd are the base materials for the FOPT and SOPT materials respectively, and the isothermal entropy change of two materials [9] are presented in Figure 2. Here an even Curie temperature distribution, $T_{Curie,n} = T_H - (T_H - T_C)(2n-1)/2n$ where n is the layer number, is expected. That is, the T_{Curie} difference between each layer is the same. Table 1 summarizes the parameters for modeling AMRs using the FOPT or SOPT materials.

Figure 3 shows the specific cooling power of the multi-layer AMRs using the FOPT or SOPT materials. Here the specific cooling power is the maximum value obtained with optimum mass flow rate. For two groups of AMRs, the specific cooling power generally increases with decreased temperature span or increased layers. Compared to the SOPT materials, although the ΔS_m peak of

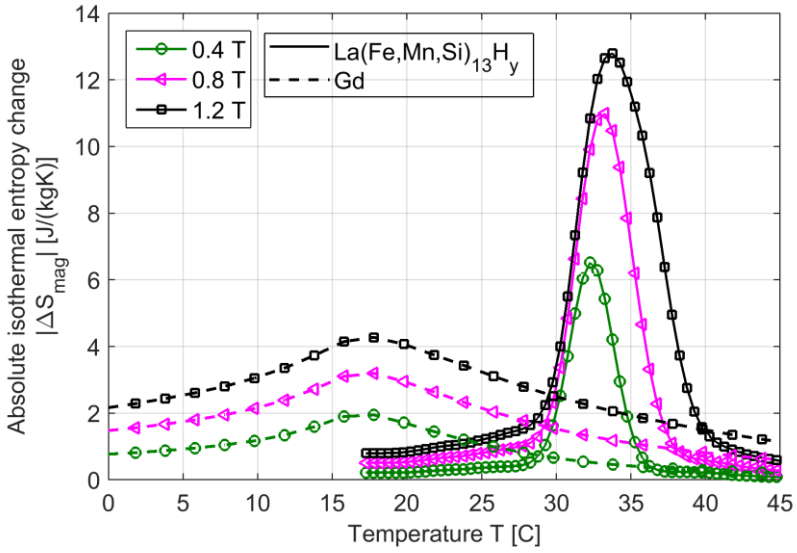

Figure 2. The absolute value of isothermal entropy change $|\Delta S_m|$ of La(Fe,Mn,Si)$_{13}$H$_y$ and Gd as a function of temperature [9]

Table 1. Parameters for modeling AMRs using the FOPT or SOPT materials

Parameter	Value
Maximum applied field	1.4 T
Temperature span	5-35 ºC
Frequency	2 Hz
Number of layers	1-40
Regenerator bed number	12
Cross sectional area of regenerator	625 mm^2
Regenerator length	50 mm
Bed geometry	Packed spheres
Sphere diameter	0.3 mm
Porosity	0.36
Heat transfer fluid	Aqueous solution with 20% v/v ethylene glycol
Thermal conductivity of $La(Fe,Mn,Si)_{13}H_y$	8 W/(m·K)
Density of $La(Fe,Mn,Si)_{13}H_y$	7000 kg/m^3
Thermal conductivity of Gd	11 W/(m·K)
Density of Gd	7900 kg/m^3

FOPT materials is much larger, ΔS_m rapidly decreases when the working temperature is away from T_{Curie}. Due to this, more layers are needed to cover a certain temperature span for the FOPT materials, which is also reflected in Figure 3. For AMRs using the FOPT materials more layers are necessary to get close to the theoretical specific cooling power, which is achieved when $N_L = 40$, while for the SOPT materials $N_L = 8$. However, the theoretical specific cooling power reachable with the FOPT materials is larger, especially when the temperature span is relatively small.

To show the influence of number of layers, the specific cooling power is further normalized to the theoretical specific cooling power and presented in Figure 4. Here the theoretical specific cooling power is obtained with $N_L = 40$ or $N_L = 8$ for two groups of AMRs, since little improvement is expected with even more layers. It shows that the nominal cooling power increases significantly with an increase in the number of layers, and fewer layers are needed for smaller temperature span, for both groups. It is clear, that more layers are desired for the FOPT materials to approach the maximum performance.

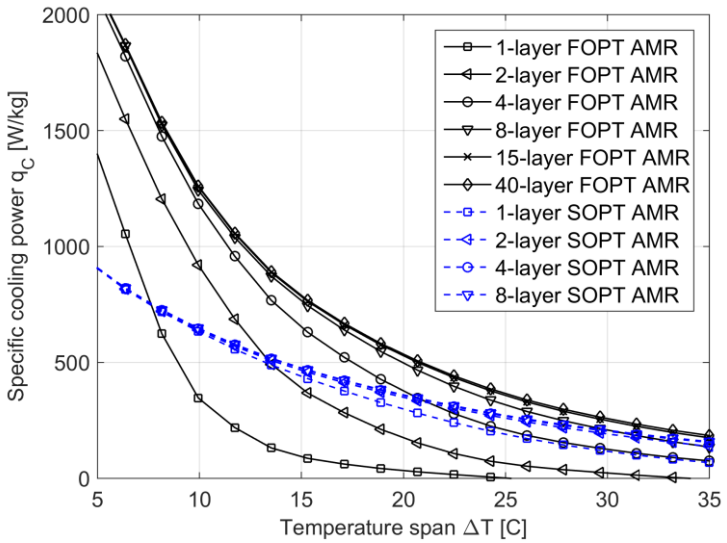

Figure 3. Specific cooling power of the multi-layer AMRs using the FOPT or SOPT materials as a function of temperature span

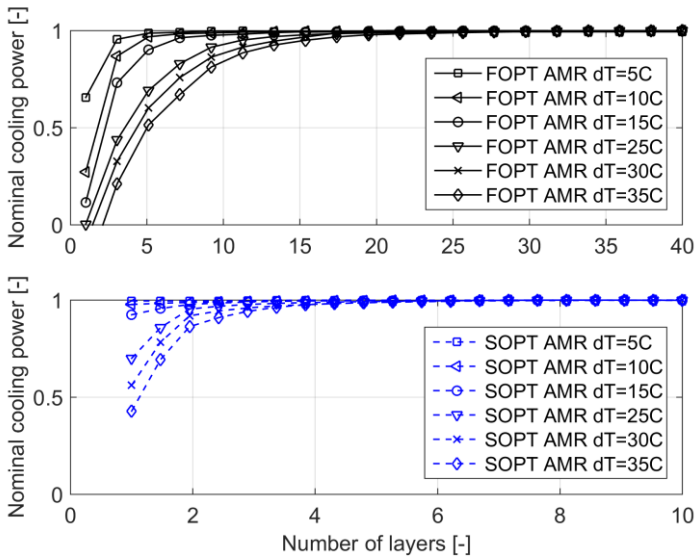

Figure 4. Nominal specific cooling power of the multi-layer AMRs using the FOPT or SOPT materials as a function of number of layers

However, building a regenerator with 40 layers may not be practical and tuning the Curie temperature with high accuracy is also difficult. Therefore, reasonable number of layers is proposed to get 90% of the theoretical specific cooling power, as shown in Figure 5. For the FOPT material, the curves of number of layers show an approximately linear relation and about 12 layers are needed with a temperature span of 35 ºC for realizing 90% maximum performance, while only 1-2 layers are necessary for the SOPT materials. It is also clear, larger specific cooling power can be obtained with the FOPT materials, and a specific cooling power of about 500 W/kg can be obtained when the temperature span is 20 ºC, while 330 W/kg for the SOPT materials.

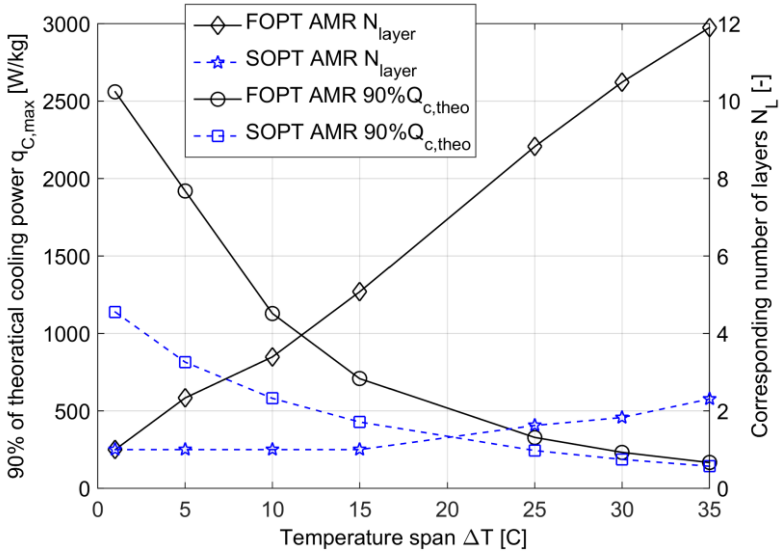

Figure 5. 90% of the theoretical maximum specific cooling power and corresponding number of layers as functions of temperature span.

3.2. Optimization of regenerator geometry and operation

In this section, we present an investigation of the influence of different geometry and operating parameters, including the aspect ratio and frequency, on the AMR performance and various loss mechanisms. Table 2 shows the modelling parameters in the simulation. Gd is used as the refrigerant and water mixture with 20 % v/v ethylene glycol as the heat transfer fluid. Here the

regenerator volume is held constant and the aspect ratio $R_a = L/\sqrt{A_c}$ can fully describe the regenerator shape. The flow rate is always optimized to get the specific cooling power of 100 W/kg for maximum the efficiency. In this way, the frequency becomes the only operating parameter to be optimized.

Table 2. Parameters for optimizing AMR geometry and operation

Parameter	Value
Maximum applied field	1.2 T
Temperature span	7 - 27 ºC
Frequency	0.3 - 10 Hz
Regenerator volume	2.25 ×10^4 mm^3
Bed geometry	Packed sphere
Number of regenerator beds	20
Aspect ratio	1.5 - 6
Hydraulic diameter	0.15 mm
Porosity	0.36
Heat transfer fluid	Aqueous solution with 20% v/v ethylene glycol
MCM	Gd

Figure 6 shows the COP of AMRs using a packed sphere bed as a function of the frequency and aspect ratio. The hydraulic diameter is 0.15 mm, corresponding to a sphere diameter of 0.43 mm. The aspect ratio ranges from 1.5 to 6 and the frequency from 0.3 to 10 Hz. It is found that the maximum COP of 6.5 can be obtained when the aspect ratio and frequency are 2.5 and 1.9 Hz, respectively. Too large or small frequency and aspect ratio leads to a significant decrease in COP.

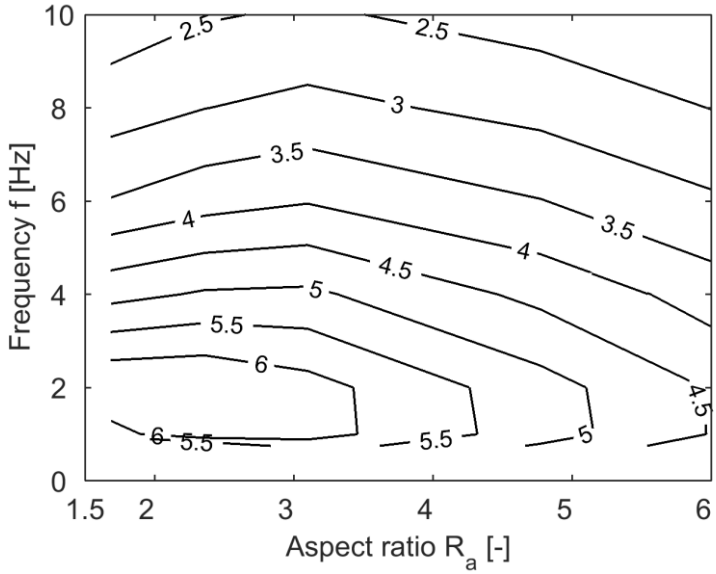

Figure 6. COP as a function of frequency and aspect ratio for AMRs using packed sphere bed with a hydraulic diameter of 0.15 mm

Figure 7a shows the total entropy production rates $\dot{S}_{p,tot}$ as a function of frequency and aspect ratio, which has a reversed pattern compared to the results of COP in Figure 6. The minimum total production rate is found at the position where the maximum COP appears. As seen in Figure 7b, the entropy production rates due to insufficient heat transfer $\dot{S}_{p,ht}$ is strongly related to the frequency rather than the aspect ratio. In contrast, the entropy production rate due to viscous dissipation $\dot{S}_{p,vd}$ in Figure 7c is more sensitive to the aspect ratio than the frequency. Since the axial conduction loss

increases when the cross sectional area becomes larger and the length shorter, $\dot{S}_{p,ac}$ increases significantly with decreasing aspect ratio, however the frequency does not affect $\dot{S}_{p,ac}$ much. In most cases, the entropy production rates representing insufficient heat transfer and viscous dissipation contribute most to the total entropy production rate, whereas the entropy production rate due to axial conduction becomes significant when the aspect ratio is smaller than 2.0. At the point of minimum total entropy production rate, the insufficient heat transfer contributes the most; the second is the viscous dissipation, while the last is axial conduction.

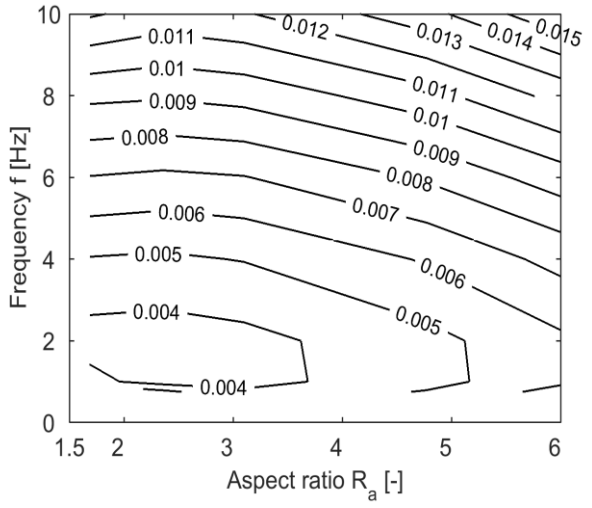

(a) Total entropy production rate consisted by three parts $\dot{S}_{p,tot}$

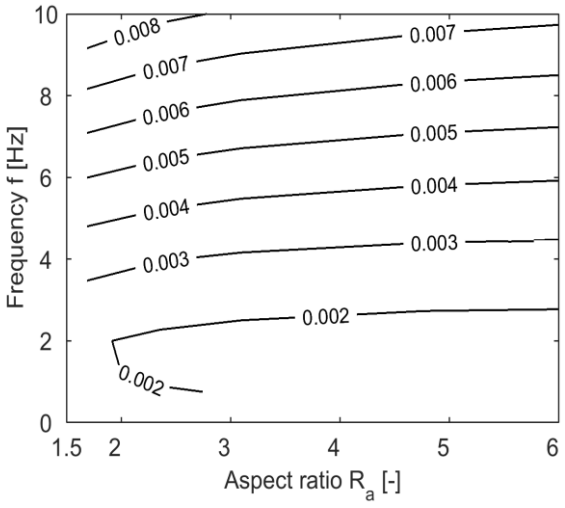

(b) Entropy production rate due to insufficient heat transfer $\dot{S}_{p,ht}$

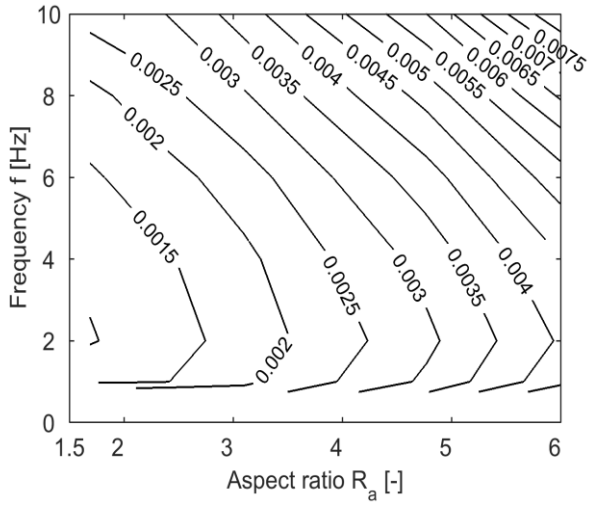

(c) Entropy production rate due to viscous dissipation $\dot{S}_{p,vd}$

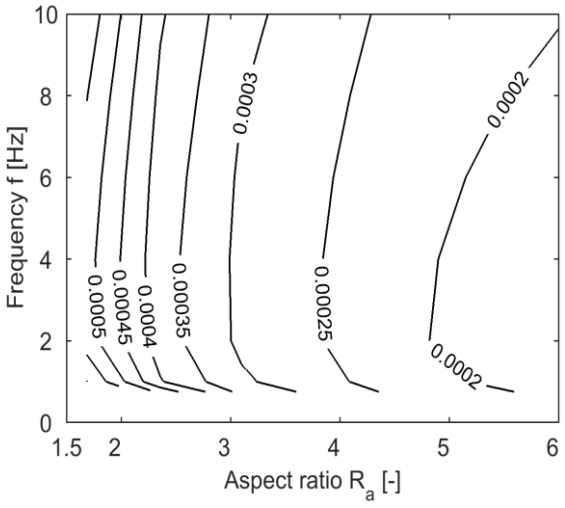

(d) Entropy production rate due to axial conduction $\dot{S}_{p,ac}$

Figure 7. Entropy production rates as a function of frequency and aspect ratio of AMRs using packed sphere bed with a hydraulic diameter of 0.15 mm

3.3. Optimization of heat transfer fluids

Increasing the heat transfer coefficient is beneficial for improving the AMR performance. In general reducing the hydraulic diameter of the regenerator bed could increase the overall heat transfer coefficient; however, it raises the risk of high viscous dissipation and overpressure due to too small channels. An alternative approach is to use a heat transfer fluid with high conductivity and low viscosity. Compared to aqueous solution with anti-corrosion additives and pure water, nanofluids may have higher thermal conductivity and convective heat transfer coefficient [11]. By adjusting the concentration of particles, the dynamic viscosity of a nanofluid can be controlled to an acceptable level. In this section, the performance of AMRs using different heat transfer fluids; water, aqueous solution with 20% v/v ethylene glycol and nanofluid containing TNS, are presented and compared.

The modeling parameters are presented in Table 1 and an AMR using a one-layer Gd regenerator is simulated. The temperature span and the frequency are 20 ºC and 2 Hz, respectively. Ref. [14] shows that the enhancement in heat transfer coefficient with nanofluids compared to water lies between 10 to 15% in the packed bed. Therefore, in the simulation, the heat transfer coefficient with nanofluid is assumed 1.1 times that of the original correlations as shown in Ref. [12]. The thermal conductivity and the dynamic viscosity of nanofluid are considered 0.6 W/(m·K) and 0.001 Pa·s respectively. The predicted specific cooling powers of AMRs using different heat transfer fluids are presented in Figure 8. The results show that the nanofluid presents the best performance with a peak value of 341 W/kg, which is higher than 325 or 302 W/kg for the other two fluids. Correspondingly, Figure 9 shows the COP of AMRs using three heat transfer fluids, and the nanofluid also exhibits the highest efficiency. Combined with the anti-corrosion additives, the nanofluid could be a promising heat transfer fluid for further improving the AMR performance.

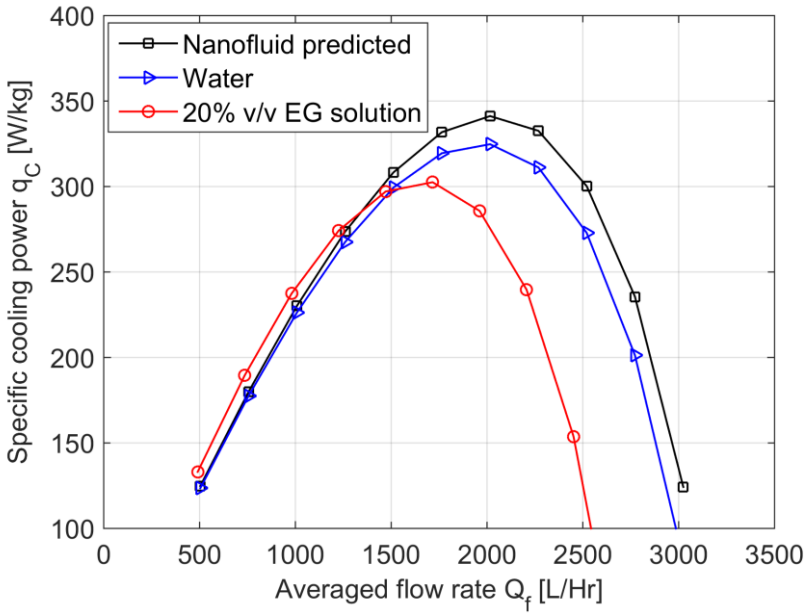

Figure 8. Specific cooling power as a function of average flow rate for AMRs using different heat transfer fluids

4. Conclusions

A 1D transient numerical model for simulating the multi-layer AMRs and an experiment apparatus for testing the heat transfer fluids in passive regenerators were developed and presented. Based on

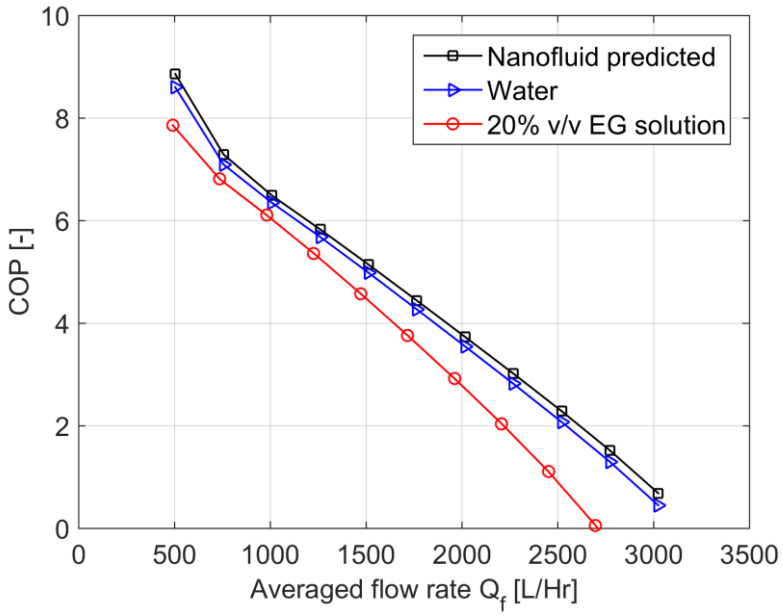

Figure 9. COP as a function of average flow rate for AMRs using different heat transfer fluids

the simulation, the influences of the number of layers and temperature span on the performance of AMRs using the FOPT or SOPT materials are quantified and compared. The results show that more layers are necessary to approach the theoretical specific cooling power for AMRs using the FOPT materials. The theoretical specific cooling power reachable with the FOPT materials is significantly lager, especially when the temperature span is relatively small, which is important for designing a compact refrigeration system. Further, a reasonable number of layers, that is 12 layers for a temperature span of 35 ºC, is proposed to get 90% of the theoretical specific cooling power for AMRs using the FOPT material. A multi-parameter optimization for maximizing the efficiency is presented combined with the method of entropy production minimization. It shows the insufficient heat transfer and viscous dissipation contribute the most and the axial conduction is less important. The performance of AMRs using three heat transfer fluids, which are water, aqueous solution with 20% v/v ethylene glycol and nanofluid, are predicted and compared. The results of the specific cooling power and the COP show that the nanofluid presents the best performance, which indicates that nanofluid could be a promising heat transfer fluid for future MCR devices.

Acknowledgments

This work was financed by the ENOVHEAT project which is funded by Innovation Fund Denmark (contract no 12-132673). The authors would like to thank Vacuumschmelze GmbH & Co., Germany for providing the $La(Fe,Mn,Si)_{13}H_y$ material.

Nomenclature

a_s	specific surface area, 1/m
A_c	cross sectional area, m^2
B	applied magnetic field, tesla
c	specific heat capacity, J/(kg·K)
c_H	specific heat capacity of magnetocaloric material at constant magnetic field, J/(kg·K)
d_h	hydraulic diameter, m
f	frequency, Hz
h	specific enthalpy, J/kg
H	internal magnetic field, tesla
k	thermal conductivity, W/(m·K)

k_{disp}	thermal conductivity of the fluid due to axial dispersion, W/(m·K)
k_{stat}	static thermal conductivity of regenerator and fluid, W/(m·K)
L	regenerator length, m
$\dot{m}_f$	mass flow rate, kg/s
n	layer number
N_L	number of layers
Nu	Nusselt number
P	pressure, Pa
$\dot{q}_C$	specific cooling power, W/kg
$\dot{Q}_f$	average flow rate, L/Hr
R_a	aspect ratio
s_s	specific entropy of solid refrigerant, J/(kg·K)
S	Entropy
$\dot{S}_{p,ac}$	entropy production rate due to axial conduction, W/K
$\dot{S}_{p,ht}$	entropy production rate due to insufficient heat transfer, W/K
$\dot{S}_{p,vd}$	entropy production rate due to viscous dissipation, W/K
$\dot{S}_{p,tot}$	total entropy production rate, W/K
t	Time, s
T	temperature, ºC
u	specific internal energy, J/kg
V_r	regenerator volume, m^3
x	axial position, m

Abbreviations

AMR	active magnetic regenerator
COP	coefficient of performance
FOPT	first order phase transition
MCM	magnetocaloric material
MCR	magnetocaloric refrigeration
NTU	number of transfer units
SOPT	second order phase transition

Greek symbols

μ	dynamic viscosity, mPa·s
ρ	density, kg/m^3
ε	porosity
τ	cycle period, s
Δ	increment

Subscripts and superscripts

ad	adiabatic process
Curie	Curie temperature
C	cold end
f	fluid
H	hot end
m	magnetic
s	solid

References

[1] Tura A., Rowe A., Progress in the characterization and optimization of a permanent magnet magnetic refrigerator. Proceedings of the Third International Conference on Magnetic Refrigeration at Room Temperature, 2009.

[2] Engelbrecht K., Eriksen D., Bahl C. R. H., Bjørk R., Geyti J., Lozano J. A., Nielsen K. K., Saxild F., Smith A., Pryds N., Experimental results for a novel rotary active magnetic regenerator. International Journal of Refrigeration 2012;(35): 1498-1505.

[3] Jacobs S., Auringer J., Boeder A., Chell J., Komorowski L., Leonard J., Russek S., Zimm C., The performance of a large-scale rotary magnetic refrigerator. International Journal of Refrigeration 2014;(37):84-91.

[4] Eriksen D., Engelbrecht K., Bahl C. R. H., Bjørk R., Nielsen K. K., Insinga A. R., Pryds N., Design and experimental tests of a rotary active magnetic regenerator prototype. International Journal of Refrigeration 2015;(58):14-21.

[5] Kitanovski A., Tušek J., Tomc U., Plaznik M., Ozbolt M., Poredoš A., Magnetocaloric Energy Conversion: From Theory to Applications. Springer 2014.

[6] Gschneidner Jr. K. A., Pecharsky V. K., Tsokol A. O., Recent developments in magnetocaloric materials. Reports on Progress in Physics 2005;(68):1479-1539.

[7] Smith A., Bahl C. R. H., Bjørk R., Engelbrecht K., Nielsen K. K., Pryds N., Materials challenges for high performance magnetocaloric refrigeration devices. Advanced Energy Materials 2012;(11):1288-1318.

[8] Barclay J. A., Theory of an active magnetic regenerative refrigerator. NASA Conference Publication, 1983:375-387.

[9] Lei T., Nielsen K. K., Engelbrecht K., Bahl C. R. H., Neves Bez H., Veje C. T., Sensitivity study of multi-layer active magnetic regenerators using first order magnetocaloric material $La(Fe,Mn,Si)_{13}H_y$. Journal of applied physics 2015;118(1):014903.

[10] Lei T., Engelbrecht K., Nielsen K. K., Veje C. T., Study of geometries of active magnetic regenerators for room temperature magnetocaloric refrigeration. Applied Thermal Engineering, 2015, in print.

[11] Wang X., Mujumdar, A. S., Heat transfer characteristics of nanofluids: a review. International journal of thermal sciences 2007;(46):1-19.

[12] Nielsen K. K., Engelbrecht K., Bahl C. R. H., The influence of flow maldistribution on the performance of inhomogeneous parallel plate heat exchangers. International Journal of heat and Mass transfer 2013;(60):432-439.

[13] Li P., Gong M., Wu J., Geometric optimization of an active magnetic regenerative refrigerator via second-law analysis. Journal of applied physics 2008;104(10):103536.

[14] Srinivasa Rao G., Sharma K. V., Chary S. P., Bakar R. A., Rahman M. M., Kadirgama K., Noor M. M., Experimental study on heat transfer coefficient and friction factor of Al_2O_3 nanofluid in a packed bed column. Journal of Mechanical Engineering and Sciences 2011;(1): 1-15.